Archives of Biochemistry and Biophysics 525 (2012) 102–110

Contents lists available at SciVerse ScienceDirect

Archives of Biochemistry and Biophysics

journal homepage: www.elsevier.com/locate/yabbi

Review

Thirty years of heme catalases structural biology

Adelaida Díaz [a], Peter C. Loewen [b], Ignacio Fita [a], Xavi Carpena [a,c,*]

[a] Institut de Biologia Molecular de Barcelona (CSIC) and IRB Barcelona, Parc Científic de Barcelona, Baldiri i Reixac 10-12, 08028-Barcelona, Spain
[b] Department of Microbiology, University of Manitoba, Winnipeg MB, Canada R3T 2N2
[c] Institut Químic de Sarrià (IQS), Universitat Ramon Llull, Via Augusta 390, 08017 Barcelona, Spain

ARTICLE INFO

Article history:
Available online 23 December 2011

Keywords:
Catalase
Heme proteins
X-ray protein crystallography
Catalase–peroxidase
KatG

ABSTRACT

About thirty years ago the crystal structures of the heme catalases from *Penicillium vitale* (PVC) and, a few months later, from bovine liver (BLC) were published. Both enzymes were compact tetrameric molecules with subunits that, despite their size differences and the large phylogenetic separation between the two organisms, presented a striking structural similarity for about 460 residues. The high conservation, confirmed in all the subsequent structures determined, suggested a strong pressure to preserve a functional *catalase fold*, which is almost exclusively found in these mono-functional heme catalases. However, even in the absence of the *catalase fold* an efficient catalase activity is also found in the heme containing catalase-peroxidase proteins. The structure of these broad substrate range enzymes, reported for the first time less than ten years ago from the halophilic archaebacterium *Haloarcula marismortui* (HmCPx) and from the bacterium *Burkholderia pseudomallei* (BpKatG), showed a heme pocket closely related to that of plant peroxidases, though with a number of unique modifications that enable the catalase reaction. Despite the wealth of structural information already available, for both monofunctional catalases and catalase-peroxidases, a number of unanswered major questions require continuing structural research with truly innovative approaches.

Introduction

Bovine liver catalase (BLC),[1] a heme containing enzyme, was one of the first proteins to be crystallized [1]. However, the first X-ray crystal structures of catalases, from *Penicillium vitale* (PVC) and BLC (at 3.5 and 2.5 Å resolution, respectively), were obtained only much later in 1980–1981, about thirty years ago, when protein crystallography had already a well established methodology and new catalase crystal forms, better suited for structural studies, had become available [2–5]. Those first catalase structure determinations represented some of the largest proteins solved at that time and provided a high resolution three dimensional framework for one of the most extensively characterized enzymes (Fig. 1). Since those initial studies many heme containing mono-functional catalase structures have been determined (Table 1), including very recently one corresponding to one of the BLC crystal forms (Form III) reported more than sixty years ago [6].

In 1979 the first catalase–peroxidase, HPI from *Escherichia coli*, was purified and biochemically characterized as a bi-functional heme containing enzyme having catalase activity [7]. The sequence of its encoding gene, katG, provided in 1988 the first catalase–peroxidase sequence, which showed a close relationship to plant peroxidases [8]. Attempts to crystallize HPI from *E. coli*, commenced in 1987, have succeeded only with its C-terminal domain [9] and the first catalase–peroxidases structures reported were from the halophilic archaebacterium *Haloarcula marismortui* (HmCPx), at 2.0 Å resolution [10], and from the bacterium *Burkholderia pseudomallei* (BpKatG) at 1.7 Å [11]. Since those structure determinations, the catalase–peroxidase structures from two other organisms have been solved (Table 2): the *Mycobacterium tuberculosis* enzyme (MtKatG), responsible for the activation of the widely used antitubercular drug isoniazid (INH) [12,13] and the catalase–peroxidase from *Synechococcus elongatus* (PDB code 1UB2).

The overall reaction characteristic of catalases is the degradation of two molecules of hydrogen peroxide giving two molecules of water and one molecule of oxygen. This apparently simple process is performed as a two-stage catalytic mechanism by all heme-containing catalases. In the first step, shared also by heme peroxidases, the first molecule of hydrogen peroxide oxidizes the heme to an oxyferryl species, named Compound I (Cpd I), where one oxidation equivalent is removed from the iron and one, generally, from the porphyrin ring and with the concomitant production of a water molecule. In the next or *catalatic* step, the second molecule of hydrogen peroxide reduces Cpd I regenerating the resting-state of the enzyme and releasing oxygen and a second

* Corresponding author at: Institut de Biología Molecular de Barcelona (CSIC) and IRB Barcelona, Parc Científic de Barcelona, Baldiri i Reixac 10-12, 08028-Barcelona, Spain. Fax: +34 93 4034979.
E-mail address: xcvcri@ibmb.csic.es (X. Carpena).

[1] *Abbreviations used*: INH, Isoniazid or Isonicotinic Hydrazide; Cpd I, Compound I; Cpd I*, Compound I*; Cpd II, Compound II.

0003-9861/$ - see front matter © 2012 Elsevier Inc. All rights reserved.
doi:10.1016/j.abb.2011.12.011

water molecule. Despite the common catalytic features, there are great differences in reactivity among the two families of heme catalases and even within each family.

Fig. 1. Wooden structure of PVC at 6.0 Å resolution [2].

A number of reviews including structural considerations are available for heme catalases, in particular for the mono-functional enzymes [14–20] but also a very detailed one for catalase–peroxidases [21]. We summarize here the main structural features and the many questions that remain unanswered for both the mono- and the bi(multi)-functional heme catalases. Other heme proteins with minor *catalatic* activity, like most mono-functional peroxidases or met-hemoglobin, will be only referenced for comparative purposes with the catalase–peroxidase enzymes. The structure of the catalytically versatile heme-thiolate haloperoxidase, with a significant catalase activity and a cysteine as the proximal ligand but a limited distribution in nature [22,23] will not be considered here. Similarly, the structure of Mn-catalases not containing the heme group will not be analysed [24]. The title of this article has been chosen, at least in part, to emphasize the complementarity and the analogies with the review of Poulos "Thirty years of heme peroxidases structural biology" also published in ABB [25].

Structures of Heme-containing mono-functional catalases

Overall structure of catalases

Heme-containing mono-functional catalases are widely distributed among aerobic organisms from bacteria, archaea and eukarya. A division into three clades of these heme catalases has been attributed to a minimum of two gene duplication events [26]. Clade 1 catalases, with ~500 residues per subunit, are predominantly of plant origin, with a subgroup of bacterial origin. The structures of only two clade 1 catalases, both from bacterial origin, are presently available (Table 1). The purification of sufficient plant catalase protein for structural determination has so far eluded success possibly a result of the largely hydrophobic exterior of the tetramer combined with the presence of surface cysteines (Loewen et al., unpublished results). Clade 2 catalases are large subunit enzymes, with ~750 residues per subunit, mostly from bacterial or fungal origin, but also present in a few archaea, likely as a result of horizontal transfer events. The structures of four clade 2 catalases have been determined (Table 1) together with a large number of variants of one of them (HPII of *E. coli*) [17]. Finally, clade 3 catalases are small subunit (~500 residues) enzymes with many structures in the PDB. These catalases are present in bacteria, archaea, fungi and many

Table 1
Representative mono-functional heme catalase structures.

PDB ID (Reference)	Catalase	Organism	Deposition Date	Res. (Å)	Clade	Heme type/orientation	Comment
4CAT [64]	PVC	*Penicillium vitale* (*P. janthinellum*)	Feb-1983	3.0	2	*b* (*) His-IV	Native
7CAT [65]	BLC	*Bos taurus*	Nov-1984	2.5	3	*b* His-III	Native
1IPH [66]	HPII/KatE	*Escherichia coli*	Dec-1995	2.8	2	*d* His-IV	Native
1A4E [67]	CAT-A	*Saccharomyces cerevisiae*	Jan-1998	2.4	3	*b* His-III	Azide complex
1DGF [39]	HEC	*Homo sapiens*	Nov-1999	1.5	3	*b* His-III	Native
1GGF [35]	HPII	*Escherichia coli*	Aug-2000	2.3	2	*b* His-IV	H2O2 complex
1HBZ [68]	MLC	*Micrococcus lysodeikticus* (*M. luteus*)	Apr-2001	1.5	3	*b* His-III	Native
1GWE [28]	MLC	*Micrococcus lysodeikticus* (*M. luteus*)	Mar-2002	0.88	3	*b* His-III	High Res.
1GWF [28]	MLC	*Micrococcus lysodeikticus* (*M. luteus*)	Mar-2002	2.0	3	*b* His-III	Cpd II
1M7S [69]	CAT-F	*Pseudomonas syringae*	Jul-2002	1.8	1	*b* His-IV	Native
1M85 [81]	PMC	*Proteus mirabilis*	Jul-2002	2.0	3	*b* His-III	Native
1QWM [48]	HPC	*Helicobacter pylori*	Sep-2003	1.6	3	*b* His-III	Formic Acid complex
1SI8 [70]	EFC	*Enterococcus faecalis*	Feb-2004	2.3	3	*b* His-III	Native
1SY7 [71]	CAT-1	*Neurospora crassa*	Apr-2004	1.7	2	*b* His-IV	Native
1YE9 [72]	HPII/KatE	*Escherichia coli*	Dec-2004	2.8	2	*b* His-IV	Truncated form
2IUF [47]	PVC	*Penicillium vitale* (*P. janthinellum*)	Jun-2006	1.7	2	*d* His-IV	Cpd I
2J2M [73]	EOC	*Exiguobacterium oxidotolerans*	Aug-2006	2.4	1	*b* His-IV	Native
2ISA [74]	VSC	*Vibrio salmonicida*	Oct-2006	2.0	3	*b* His-III	Native
2IQF [47]	HPC	*Helicobacter pylori*	Oct-2006	1.9	3	*b* His-III	Cpd I
3EJ6 [75]	CAT-3	*Neurospora crassa*	Sep-2008	2.3	2	*b* His-IV	Native
2XF2 [76]	PVC	*Penicillium vitale* (*P. janthinellum*)	May-2010	1.8	2	*d* His-IV	Aminotriazole complex
2XQ1 [77]	PAC	*Pichia angusta*	Aug-2010	2.9	3	*b* His-III	Native

* Originally traced as Heme *b*, was later confirmed to be Heme *d*.

Table 2
Representative catalase–peroxidase structures.

PDB ID (Reference)	Catalase	Organism	Deposition date	Resolution (Å)	Comment
1ITK [10]	HmKatG	*Haloarcula marismortui*	Jan-2002	2.0	Native
1MWV [11]	BpKatG	*Burkholderia pseudomallei*	Oct-2002	1.7	Native
1UB2 [Not published]	SeKatG	*Synechococcus elongatus*	Mar-2003	2.4	Native
1SJ2 [13]	MtKatG	*Mycobacterium tuberculosis*	Mar-2004	2.4	Native
1X7U [78]	BpKatG	*Burkholderia pseudomallei*	Aug-2004	1.9	Mutant S324T
2B2S [58]	BpKatG	*Burkholderia pseudomallei*	Sep-2005	2.0	Cpd I
2CCA [79]	MtKatG	*Mycobacterium tuberculosis*	Jan-2006	2.0	Mutant S315T
2FXG/H/J [80]	BpKatG	*Burkholderia pseudomallei*	Feb-2006	2.0/1.9/1.9	Native pHs 4.5/6.5/8.5
3N3O [56]	BpKatG	*Burkholderia pseudomallei*	May-2010	1.7	NAD-Native complex
3N3Q [56]	BpKatG	*Burkholderia pseudomallei*	May-2010	1.9	INH-S324T complex

other eukaryotes including mammals, but absent in older taxonomic groups suggesting that they arose later in evolution.

Catalase subunits from the three clades present very high structural similarities for about 460 residues, even among the enzymes from the most distantly related organisms, with root mean square deviations (rmsd) for C^{α} atoms of only ~1 Å. This highly conserved three dimensional organization is referred to as the *catalase fold* and it is found almost exclusively in mono-functional heme catalases (Fig. 2A and B). The *catalase fold* consists of two globular domains (the β-barrel and the α-helical domain) linked to each other by a long protein segment named the wrapping loop, which contains the helix with the tyrosine acting as the heme proximal ligand. The β-barrel domain, an anti-parallel eight-stranded β-barrel that includes also at least six inserted α-helices, is the central feature of the *catalase fold*. The β-barrel domain is preceded by an extended N-terminal arm and followed by the wrapping loop and the α-helical globular domain. The first half of the barrel (β1–β4) contains most of the residues that define the heme distal side, while the second half (β5–β8) contributes to the NADP(H) binding pocket in those catalases that bind the nucleotide (see below). The quaternary organization of catalases is also very well preserved with compact tetramers organized with accurate **D2** molecular symmetry and presenting an intricate intersubunit threading of the amino terminal arm of one subunit through the wrapping loop of a neighbour subunit, which seems to require a close coordination between the folding and the oligomerization of subunits [17] (Fig. 2C). Oligomerization appears to be part also of the heme internalization process and the heme cavity involves residues from two different subunits. The large size of clade 2 catalase subunits is due to the presence of a conspicuous C-terminal domain of ~150 residues. This extra domain, less well conserved than the *catalase fold*, has a "flavodoxin-like" topology that belongs to the type 1 glutamine amidotransferase family [27] though no nucleotide binding to this domain has been reported and other possible roles remain uncertain. In many catalase structures the molecular symmetry necessarily breaks at least at one point along the two fold axis [28] suggesting that a subtle departure from perfect symmetry could be useful for the functioning of the enzyme, although this has not so far been confirmed (Jha et al., in this volume).

Heme, heme pocket and heme channels in catalases

The heme orientation, defined by the position of vinyl and methyl groups from the pyrrole rings I and II, appears well established for a given catalase (Fig. 3). However, the two possible heme orientations have been observed in different catalases, which results in the essential catalytic histidine (His128 in HPII) above either pyrrole ring III or IV (indicated in Table 1 as His-III or His-IV, respectively). The clade 1 and all the clade 2 catalase structures determined present the His-IV orientation, while all clade 3 structures present the "flipped" orientation His-III. The analysis of residues in contact with the two methyl and the two vinyl groups suggests that the distribution of heme orientations will be maintained according to their clade for most enzymes, in particular from clade 2 [18]. However, both orientations have been found in

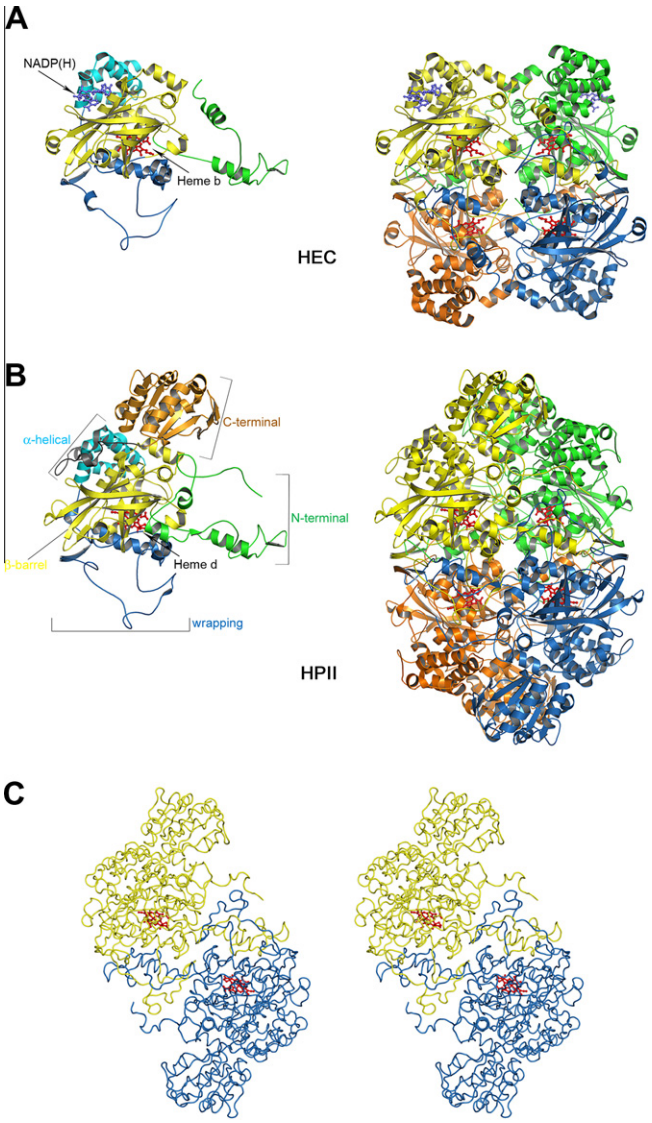

Fig. 2. Catalase structures. Views of the subunit (left) and of the tetrameric molecule (right) of (A) human erythrocyte catalase (HEC) and of (B) catalase from *Escherichia coli* (HPII), as representative examples of small and large catalases, respectively. (C) Stereo view of the two HPII subunits that participate in the threading of the N-terminal arm throughout the wrapping loop of the neighbour subunit.

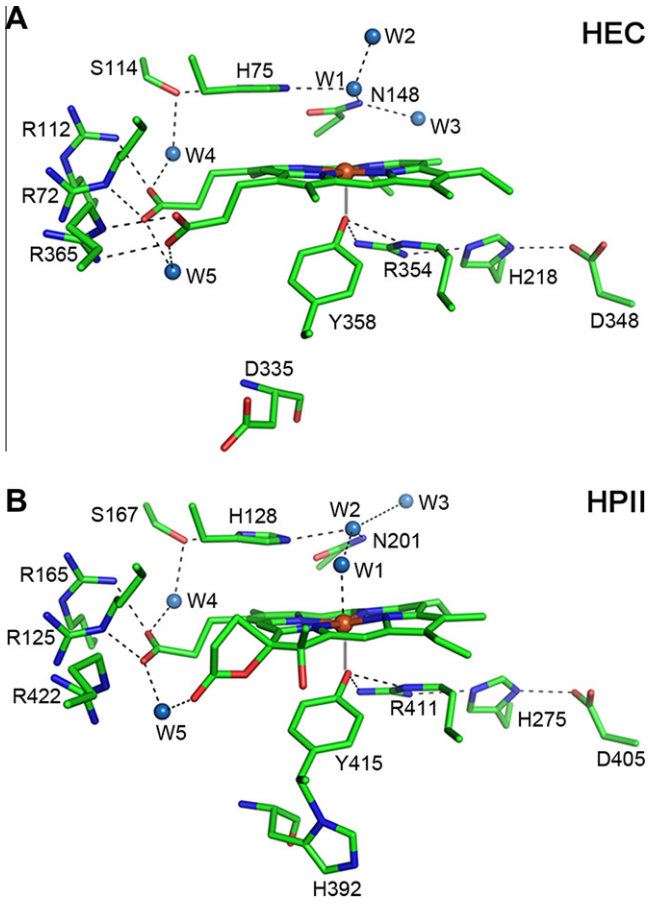

Fig. 3. Heme environment in catalases. Heme environment in (A) human erythrocyte catalase (HEC) and (B) catalase HPII from *Escherichia coli*. HEC contains heme *b* with the His-III orientation while HPII contains heme *d* with the His-IV orientation. The essential distal histidine in catalases (His75 in HEC or His128 in HPII), with the imidazole moiety stacked on the heme ring, differs from peroxidases where the imidazole is perpendicular to the heme ring. Notice also in HPII the existence of a covalent bond between the proximal tyrosine (Tyr415) side chain CB atom and the side chain of His392.

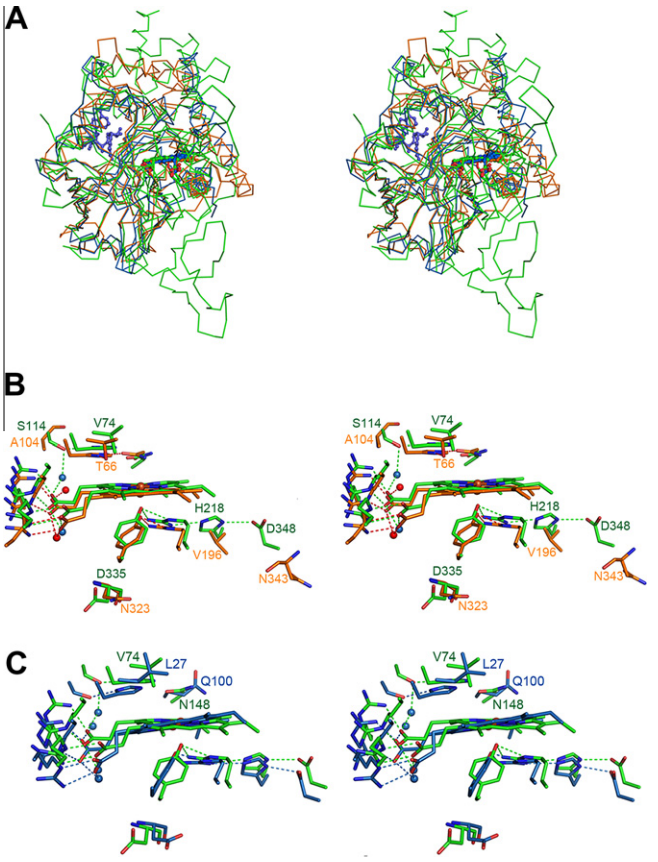

Fig. 4. Structural comparisons of catalase folds. (A) Stereo view of the overall superimposition of the "catalase folds" from Human Erythrocyte Catalase HEC (green), with the hemoproteins allene oxide synthase from the coral *Plexaura homomalla* (orange) and the peroxidase from *Mycobacterium avium* ssp. *paratuberculosis* annotated as MAP-2744c (blue). Superimpositions of the active centers of HEC with the allene oxide synthase (B) and with the peroxidase MAP-2744c (C).

the Ile274 variants of HPII when the bulky isoleucine, adjacent to the heme, is exchanged by smaller side chains [29] suggesting that even residues not in direct contact with the methyl or vinyl groups can affect the orientation of the heme.

At least four covalent variants of the heme group, which is not covalently bound to the polypeptide, have been reported in catalases: the heme *b* itself (ferriprotoporphyrin IX), the heme *d* found in some large catalases, and the heme degradation pigments biliverdin or bilirubin. Heme *d*, a *cis*-hydroxyspirolactone formed between the propionic group and the pyrrole ring away from the essential histidine, has been found only in some clade 2 enzymes. In fact, heme *d* was present in the first catalase crystal structure determined of PVC, though its identity was not recognized till much later simultaneously with the recognition of heme *d* also in HPII [30]. In HPII, His392 forms a covalent bond with the proximal tyrosine (Fig. 4). His392Gln variant contains exclusively heme *b*, whereas His392Glu contains a mixture of *cis* and *trans* isomers of heme *d*. Heme *d* is produced as a specific self modification of the heme *b* during the first cycles of enzymatic activity [31,32] likely to increase the stability of Cpd I in those catalases as the heme modification is not required for activity. Instead heme degradation pigments seem to be the result of unspecific side effects of the enzyme activity [33] and their content varies widely among different catalases. Indeed, there is even variation between tissue source with ~100% heme *b* in the erythrocyte enzyme and up to ~50% degraded heme in the liver enzyme.

Heme pockets are extremely well preserved among different catalases, though only three residues were initially defined as essential for catalysis: the proximal ligand tyrosine (Tyr 415 in HPII) and the catalytic histidine and an asparagine on the heme distal side (His128 and Asn201 in HPII, respectively) [34]. The structural analysis indicated that several other residues, such as the arginine interacting with the proximal tyrosine (Arg411 in HPII), the serine interacting with the essential histidine (Ser167 in HPII), and some residues in the heme channels, such as an aspartate in the lower part of the main channel (Asp181 in HPII), could also have a critical role in catalysis. In turn, variants of the "essential" asparagine retain some significant activity questioning its "essential" contribution to catalysis [35] that, molecular dynamic studies suggest, can be related mainly with the orientation and flow of substrates and products [36,37].

Heme groups are deeply buried inside the catalase tetramers, with the heme iron atoms at more than 20 Å from the nearest molecular surface, which raises a number of intriguing questions related to the heme internalization and, in particular, the substrates entering into and products releasing from the heme pocket. Several possible channels connect the heme with the protein surface. The main channel, so named because it is the most obvious access route to the heme, has long been considered the primary access route for the hydrogen peroxide substrate, a concept supported by molecular dynamic studies [36]. A comparison of the main channels in small and large catalases showed the extended

and bifurcated structure in large catalases as compared with the shorter funnel shape in the small enzymes. An extensive analysis of the waters occupying the main channels reveals a number of consistently occupied sites as well as a number of sites that consistently present low occupancies [38]. The lack of waters in a hydrophobic portion of the channel, between a conserved aspartate (Asp181 in HPII) and the essential histidine, was interpreted as a "molecular ruler" optimized to select hydrogen peroxide [39]. This could be complemented by the electrical potential in the channel, between the negatively charged conserved aspartate and the positively charged heme iron, acting on the electrical dipoles of the incoming hydrogen peroxide molecules orienting them favourably for immediate reaction upon entering the heme cavity [38]. This would result in a "chain-like reaction" process consistent with both the high values of the (apparent) K_M of catalases for H_2O_2 and the fast turnover rate of the catalatic reaction [16]. A highly conserved four residue loop above the hydrophobic portion of the channel has been proposed to act, in large catalases, as a gate accessible through either the main channel or an interconnection with the gate from another subunit. Molecular dynamics with *Neurospora crassa* catalase-1 has shown that the number of H_2O_2 molecules found both at the protein surface and at the vicinity of this gate is higher compared to other catalases due to the presence of aminoacids that have an increased residency for H_2O_2 (mainly histidine, proline and charged residues). Therefore, it seems that catalases have mechanisms to increase the local concentration of hydrogen peroxide that affect the catalytic efficiency [40]. Related with this, the HPII variants of Ile274 with smaller residues exhibited lowered activity consistent with retention of substrate molecules in the heme cavity being a prerequisite for the second stage of the catalatic process [29].

Besides the main channel other possible routes to access the heme pocket have been described including a minor or lateral channel, which approaches the heme laterally, and a channel that might connect the heme with the cavity at the molecular centre. These secondary channels might be specific for the exit of the different reaction products, a stringent requirement given the high speed of the catalase functioning. Consistent with this conjecture, enlarging the lateral channel by removing the side chain of Arg260 in HPII increases the specific activity of the variant Arg260Ala to two times that of the native enzyme [41].

NADP(H) binding to catalases

The discovery of a strong binding of NADP(H) to mammalian catalases [42] came as a most unexpected surprise since the dinucleotide cofactor was unnecessary for catalysis and the *catalase fold* did not contain a known nucleotide binding motif [19]. In fact, no NADP(H) binding has been reported to any clade 1 or 2 catalases confirming that the dinucleotide is not needed for the catalase activity. In turn, all eukaryotic and most prokaryotic clade 3 enzymes seem to bind NADP(H), though with a wide range of affinities. The NADP(H) binding site, at the interface of the β-barrel and the α-helical domains, is exposed to the solvent and associated with the entrance to the lateral channel placing the nicotinamide active carbon (C^4) about 20 Å from the heme iron atom (Fig. 2). Bound NADP(H) molecules present a compact right-handed helical conformation, with the two bases within 4 Å of each other. In some of the structures determined, the nicotinamide moiety is more disordered than the adenine part suggesting that binding to nicotinamide might be more affected by the environmental conditions and the oxidation state of the dinucleotide. The biochemical or biological roles of NADP(H) binding to catalases are not well understood, though protection against inactivation by reduction to a Compound II (Cpd II) intermediate during periods of slow catalatic turnover is currently favored [19,43]. For such a role, an electron transfer from NADPH to the heme appears necessary, which requires a model for an electron path extending from the nicotinamide moiety of the NADPH to the heme edge [44,45]. Clade 2 catalases present a segment of the protein (residues 585–590 in HPII) occupying most of the space corresponding to the NADPH binding pocket that would prevent NADPH binding [46]. However, despite the presence of the protein segment blocking the NADPH site, the entrance to the lateral channel remains there in the large catalases.

Structures of catalases complexes

The crystal structures of Cpd I in large catalases and of Cpd I* (isoelectronic with Cpd II in the vicinity of the heme) in *Micrococcus lysodeikticus* catalase (MLC), were obtained by soaking with peracetic acid (PAA) and reported at 1.8 and 1.6 Å resolution, respectively [28,47]. Both complexes confirm the absence of major structural rearrangements with respect to the resting enzymes, and the continued absence of well defined solvent molecules in the lower part of the main channel. In both complexes the iron atom is displaced towards the coordinated oxygen resulting in an oxygen-iron distance of ~1.7 Å in Cpd I. The structures of PVC and of HEC with the specific catalase inhibitor 3-amino-1,2,4-triazole (AT) show a covalent bond between the essential histidine N^{ε} atom with the C^5 atom of the inhibitor, which has all its atoms at ~3.5 Å from the heme precluding the possibility of a direct coordination with the iron [16]. Intriguingly in the structure of human erythrocyte catalase with four subunits in the crystal asymmetric unit, only two presented a bound NADP(H) molecule and AT was found only in the two subunits without NADP(H) bound [39]. The crystal structures of most catalases complexed with azide, a classical heme inhibitor, confirm the coordination of the heme iron with the azide nitrogen N1 and a Fe–N1–N2 coordination angle of ~130°, which is similar to the values found for other azide-heme complexes. Curiously, azide was found in HPC not bound at the heme but at a region along one of the two fold axes [48]. The structures of the complexes of catalase inhibited by cyanide revealed significant changes only in the heme distal pocket where cyanide is coordinated linearly to the iron with a carbon-Fe distance of ~1.60 Å [39].

Soaking crystals of the inactive His128Asn HPII variant with hydrogen peroxide, resulted in a clear departure from the **D2** molecular symmetry for some residues in the vicinity of the heme proximal tyrosine [35]. The soaking also led to the identification of several H_2O_2 molecules at specific locations within the main channel and in the distal pocket. During soaking with PAA five out of seven methionines of MLC were oxidized to methionine sulfoxide. Some of the modified methionines seem to occupy specific positions within the catalase structure either in the main heme channel or clustering with the corresponding residues from symmetry-related subunits [28,47,49].

Enzymes structurally related to catalases

The hemeprotein allene oxide synthase from the coral *Plexaura homomalla* and the peroxidase from *Mycobacterium avium* ssp. *paratuberculosis* annotated as MAP-2744c are, to our knowledge, the only other reported structures presenting the *catalase fold* besides mono-functional catalases (Fig. 4) [50,51]. The coral enzyme, found in a naturally occurring fusion protein, shows a striking structural similarity to catalases including a complete β-barrel and part of an α-helical domain, with an overall rmsd of 1.65 Å for 225 equivalent residues, despite a weak sequence identity (~10% amino acid identity). The 33-kDa peroxidase MAP-2744c retains also the β-barrel domain and the helix containing the tyrosine heme binding proximal ligand. As a result the conservation of the heme environment

with respect to catalases is remarkable for both enzymes, especially since their heme pockets are formed by residues from only one subunit. In particular, the important catalytic residues found in catalases are very precisely maintained (such as the tyrosine acting as the proximal iron ligand and interacting also with a fully conserved arginine, the histidine on the distal side and the three arginines interacting with the heme propionic groups). The "essential" asparagine found on the heme distal side of catalases is also present in the coral enzyme, but has been replaced by a glutamine, adopting a different conformation in MAP-2744c. The close similarity of the heme pockets suggests that differences in the access and exit channels to and from the heme, together with subtle changes in the heme-environment, could result in significant differences in the catalytic activities of enzymes structurally related to catalases.

Is structural research about catalases still needed?

Despite the wealth of information available, there remain a large number of structure-related important questions such as the following:

(1) What is the role of the extra C-terminal domain in large subunit catalases?
(2) Why has the *catalase fold* been so precisely preserved, in particular taking into account the small substrate size?
(3) Is there a mechanistic function for the only residue within the *catalase fold* that is in a disallowed region of the Ramachandran plot (Ile274 in HPII)?
(4) Why is the *catalase fold* present almost exclusively in monofunctional catalases?
(5) How is the threading between subunits achieved? Why has it been preserved?
(6) Could the structure of plant catalases present any structural peculiarities besides the predicted prevalence of hydrophobic and cysteine residues at the molecular surface? Do the surface cysteine residues have a role?
(7) How do substrate and product molecules flow inside the catalase channels and how might this flow be regulated? Are there discrete entrance and exit channels? In particular, are there separate exit channels for the different products of the catalase reaction, O_2 and H_2O?
(8) Can channels from different subunits interact with each other?
(9) Does NADP(H) participate in the channel regulation?
(10) Is there any cooperativity between subunits?
(11) Are asymmetric movements possible as was suggested both by the structure of the inactive HPII variant soaked with hydrogen peroxide and by the departures from perfect symmetry at certain positions in the vicinity of the molecular twofold axis?
(12) Do the conserved methionines, their accumulation at specific locations and frequent oxidation have functional roles?
(13) Do the modifications observed in HPII including the oxidation of heme *b* to heme *d* and the covalent linkage of the proximal tyrosine to a histidine have a role?
(14) Many questions related to the role and the binding of NADP(H) to catalases remain and we refer you to the review from Kirkman and Gaetani [19].

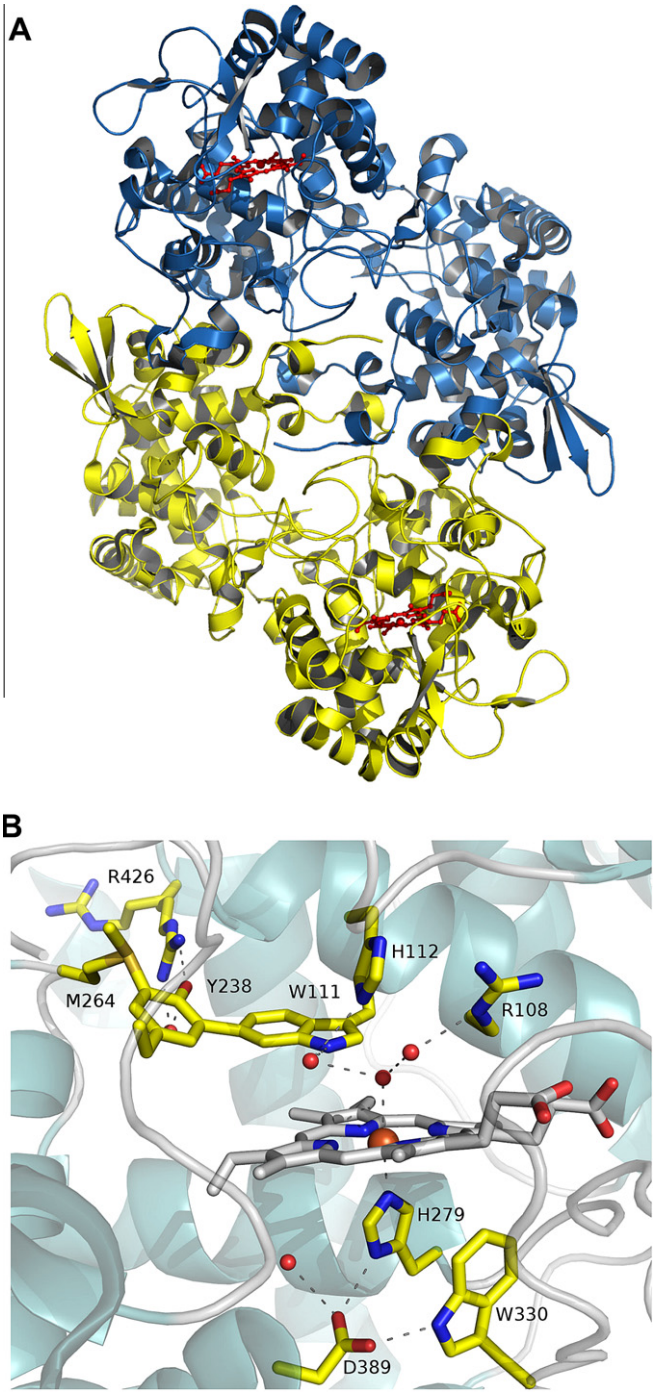

Fig. 5. The catalase–peroxidase structure. (A) View down the molecular two fold axis of the structure of *Burkholderia pseudomallei* (BpKatG) dimer. The heme group is shown as red ball-and-sticks in the two subunits. (B) Close up view of the heme pocket showing, in particular, the presence of the covalent adduct in the proximal side involving residues Met264-Tyr238-Trp111 and the mobile arginine (Arg426) represented here in the two experimentally observed conformations.

Structures of heme-containing catalases-peroxidases

Overall structure

Catalase–peroxidases are heme enzymes phylogenetically related to the superfamily of plant-fungal and bacterial peroxidases [52]. Despite having a different fold and different organization of the heme pocket compared to monofunctional catalases, they efficiently catalyze the dismutation of hydrogen peroxide in addition to the peroxidase reaction that becomes significant when a suitable organic electron donor is present, though none has been identified *in vivo*. In fact, the structural differences between catalase–peroxidases and monofunctional catalases do contribute to significant differences in catalytic properties even for the common catalatic reaction. Catalase–peroxidases apparently evolved much later than heme mono-functional catalases and are present primar-

ily in aerobic bacteria while the limited appearance in some archaea and fungi is probably a result of lateral gene transfer [18]. The crystal structures of three catalases-peroxidases from bacteria and of one from archaebacteria have been reported (Table 2).

Catalase–peroxidases are normally dimers both in the crystal structure and in solution, although HPII of *E. coli* does form a stable tetramer. In the dimer, the two subunits (of about 750 residues each) present an extensive contact surface without any significant interdigitation. Subunits are organized into separate N-terminal and C-terminal globular domains, both closely related to plant heme-peroxidases, arranged along the longest subunit axis of the molecular dimer (Fig. 5). Despite the similarities of both domains with heme-peroxidases, only the N-terminal domain contains a heme group. The C-terminal domain, which has suffered greater evolutionary drift when compared to plant peroxidases, has occluded the location corresponding to the heme pocket with a segment of the protein. The N-terminal domain of catalase–peroxidases includes also an extension of about 60 residues that is absent in plant peroxidases. This N-terminal extension is disordered for at least 30 residues in all the structures determined, likely indicating a great flexibility despite the presence of a well conserved cysteine (Cys27 in BpKatG), which might form a disulfide bridge between the two subunits of the dimer [53]. Catalase–peroxidases present also three long loops, each more than thirty residues longer than the corresponding ones in plant peroxidases, which contribute to configure a deep heme pocket.

Heme, heme pocket and heme channels

The heme *b* group in catalase–peroxidases is not covalently linked to the protein, always presents the same orientation and contains, in the resting state of the enzyme, a ferric iron that is coordinated with the N^{ε} atom from the histidine proximal ligand (His279 in BpKatG). Only one possibly labile covalent modification of the heme has been reported based on electron density maps, which seem to be consistent with a perhydroxy modification on the ring I vinyl group of the heme [11,54]. In the resting enzyme the sixth coordination site of the iron is occupied by a loosely bound water molecule at a distance of around 2.6 Å. However, this water is, at least partially, replaced in many of the structures, particularly at high pHs, by the atoms of a perhydroxy (–OOH) modification of the indole group of the nearby distal side tryptophan residue (Trp111 in BpKatG) (Fig. 5B).

The heme pocket of catalase–peroxidases is similar in most respects to that of plant peroxidases both on the proximal and distal heme sides (Fig. 5). In particular, the proximal histidine makes a hydrogen bond with an aspartate (Asp389 in BpKatG) and shows stacking interactions with a tryptophan (Trp330 in BpKatG). On the distal side, the imidazole moiety of the essential histidine is oriented perpendicular to the heme with the N^{ε} pointing towards the heme iron at a distance of ~5.5 Å, while the N^{δ} atom acts as the donor in a hydrogen bond with a conserved asparagine (Asn142 in BpKatG). An arginine (Arg108 in BpKatG) is also found in the distal side pocket of both catalases-peroxidases and plant peroxidases. A unique and striking feature found in catalase–peroxidases is a covalent adduct in which a tyrosine is linked at its ortho positions to a methionine on one side and a tryptophan on the other (Met264-Tyr238-Trp111 in BpKatG) (Fig. 5B). The structure of the tyrosine and tryptophan rings deviate from planarity suggesting the bond between them is not pure sp^2 in character. As part of the adduct the methionine is most likely carrying a positive charge that could provide a draw for electrons in the adduct. The self-catalysis of the covalent adduct has been demonstrated in catalase–peroxidases [55] but it has not been possible to obtain crystals of the protein before the modification is fully formed indicating that the adduct

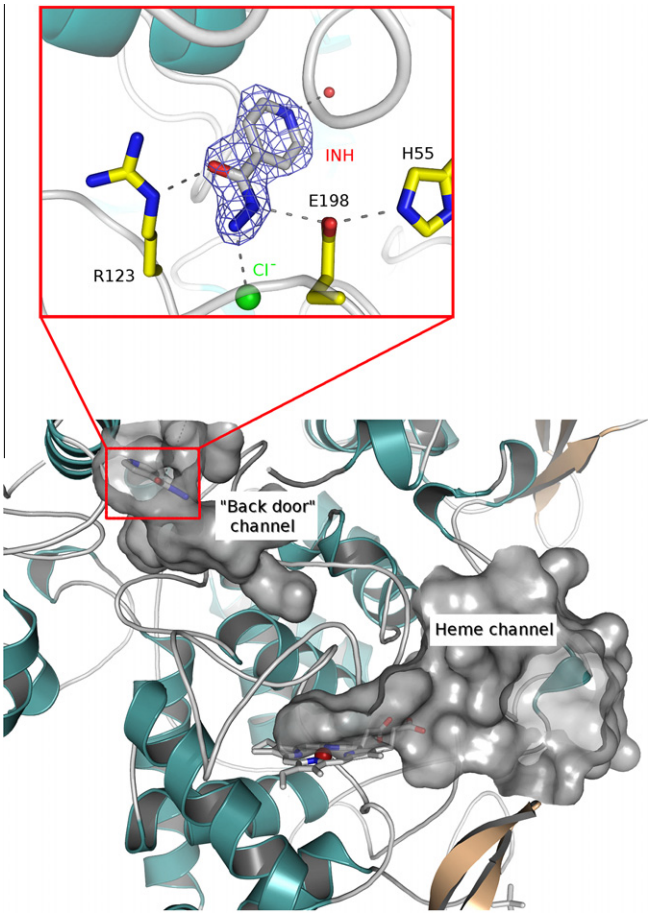

Fig. 6. Molecular channels towards the catalase–peroxidase core. The molecular surfaces corresponding to the main heme channel and to the "back door entrance", where the INH was found to bind in BpKatG, are explicitly labelled. The heme group and the INH molecule are also shown. The inset shows a detailed view of the interactions and the electron density of the INH bound molecule.

causes some changes in the larger protein. The adduct is in close association with a conserved mobile arginine (Arg426 in BpKatG) that can adopt two conformations, one of which interacts with the adduct tyrosine (Fig. 5B). The three residues from the adduct and the mobile arginine have been shown to be essential for the catalatic reaction but not for the peroxidatic processes [21].

The most obvious access route to the distal site of the heme is provided by a channel positioned similarly to, but longer and more constricted than, the access route in peroxidases (Fig. 6). This channel has a pronounced funnel shape and is narrowest just before entering the heme pocket with a continuum of water molecules clearly defined in many of the structures determined. Most peroxidases have a second access route, approximately in the plane of the heme, leading to the distal side. However, in catalase–peroxidases this second route appears to be blocked by the larger loops suggesting that substrates entering into and products releasing from the heme pocket all use the funnel shaped channel. However, there does appear to be at least one other approach to the subunit core starting at the molecular two fold-axis and approaching the neighbourhood of the mobile arginine. This possible back door entrance to KatGs has, in fact, been shown to be the binding site of chlorine and also of the antitubercular drug INH in BpKatG [56]. Removal of the distal side arginine (Arg108 in BpKatG) can also open an alternative access to the heme, which can contribute to the relevance of this residue in catalysis related with the presence of a distal side aspartate (Asp141 in BpKatG) [21,57].

Structures of catalase–peroxidase complexes

Structures of oxyferryl species of both catalases and peroxidases have been reported and a crystal of BpKatG soaked briefly with a peracetate solution proved to be similar in containing an oxygen closely coordinated to the iron [58]. While the initial oxyferryl species formed may have been a classic porphyrin cation radical Cpd I species, this was not the species evident in the electron density maps following data collection and refinement which presented a Fe–O bond length of 2.2 Å. Facile electron transfer within the protein leads rapidly to Cpd I* (protein radical Fe–OH species) with a longer Fe–O bond length expected to be ~1.8 Å, but this species proved to be sensitive to X-ray damage, like the oxyferryl form of HRP, giving rise to the long Fe–O distance. Merging images from short exposure times from three crystals shortened the apparent Fe–O distance to 1.88 Å more consistent with the expected Cpd I* species. The only other significant change in structure from the native enzyme was a shift in the position of the mobile arginine (Arg426 in BpKatG) to 100% R conformation. The changes in conformation of the mobile arginine have been rationalized in terms of modulating electron flux in the adduct and the heme and are essential for the catalase reaction to proceed.

The activation of INH by BpKatG or MtKatG involves removal of the diimide and one electron from INH to create an isonicotinyl radical, which then reacts with NAD^+. The isonicotinyl-NAD radical is then reduced to isonicotinyl-NAD, the active form of the drug, that inhibits mycolic acid synthesis [56]. The principal role played by KatGs in this process lies in the enhancement of the rate of INH breakdown to the isonicotinyl radical. Subsequent reaction of the radical with NAD^+ and reduction of the isonicotinyl-NAD radical by superoxide ion are only marginally influenced by KatG except possibly by enhanced superoxide production. The binding sites, found in complexes of BpKatG with INH and NAD^+, can be interpreted as being consistent with this mechanism [56]. INH was found at the opening of the potential back door entrance (see previous section) at about 10 Å from Trp139, a site of stable radical accumulation (Fig. 6). While the same radical sites have not been confirmed in MtKatG, INH has been shown to reduce similar protein radicals in that enzyme [59]. A BpKatG-NAD^+ complex was also crystallized leading to the identification of a NAD^+ binding site on the surface of the protein about 20 Å from the main entrance channel to the heme. This binding site was disconcerting for two reasons. The first was its significant separation from the INH binding site which suggested that one or both of the isonicotinyl radical and NAD^+ had to dissociate from their binding sites to find the other reactant. The second was that the binding site, evident only in one subunit at the surface of the protein, suggested a weak binding easily affected by crystal packing and crystallization conditions. Thus, despite NADH being a known substrate for KatG in a location where NAD^+ acts as a competitive inhibitor, the binding site for the nucleotide remains uncertain.

Modelling studies

Quantum mechanics and dynamics simulations have provided invaluable insights into the reaction mechanisms of KatGs and the possible roles of the adduct and mobile arginine in the catalatic process [60,61]. Density functional theory (DFT) calculations using quantum mechanics and molecular mechanics (QM/MM) models of an oxyferryl Cpd I species, including in the quantic description the close heme environment plus the M–Y–W adduct, suggest that spin density locates on the adduct only when the adduct tyrosine is unprotonated and the mobile arginine is not associated. Protonation or association with the mobile arginine leads to spin density moving to the proximal tryptophan (Trp330 in BpKatG) similarly to what is expected to happen in cytochrome C peroxidase [60]. Significantly, little spin density was found on the heme suggesting a relatively unstable heme radical consistent with its rapid reduction and formation of stable protein radicals in residues away from the heme such as Trp139 and Trp153 in BpKatG. These calculations were therefore suggestive of a transient protein radical being formed on the adduct and this has been adapted into a mechanism for the catalatic reaction. Experimental evidence for such a transient radical has been recently obtained [62] and the adduct radical has also been implicated in the reaction of KatGs with molecular oxygen to form the perhydroxy modification on the adduct tryptophan indole and superoxide in the presence of electron donors such as INH [61].

Open questions related with the structure-function of catalases-peroxidases

Similarly to monofunctional heme-catalases, a large number of structure-related questions about catalases-peroxidases remain unanswered despite the recently accumulated structural information. Among these questions:

(1) What is the role of the C-terminal domain [63]?
(2) How can catalase–peroxidases switch between peroxidatic and catalatic reactions?
(3) Has the catalatic reaction pathway been fully defined?
(4) Are the NAD(H) and INH binding sites found in BpKatG valid for other catalase–peroxidases, in particular for the *Mycobacterium tuberculosis* KatG enzyme?
(5) At what level do the residues where stable radicals accumulate participate in the catalytic processes?
(6) Why do the sites of stable radical accumulation differ in different catalase–peroxidases?
(7) What are the *in vivo* peroxidatic substrates of catalase–peroxidases and where on the enzyme do they bind?
(8) Does the "back door entrance" to KatGs have a function?
(9) What structural changes are introduced by the formation of the covalent adduct that facilitate crystallization?
(10) What is the role of the flexible N-terminus and of the conserved cysteine in this region? Could they participate in the formation of the reported larger oligomers such as the tetramer in HPI?
(11) Is there any cooperativity or communication between subunits?
(12) Is the flow of substrate and products to and from the heme through the narrow channel modulated in any way?
(13) Do eukaryotic catalase–peroxidases have consistent structural peculiarities?

Conclusions

About thirty years ago the first crystal structures of heme containing catalases were published showing a unique, strongly preserved, three-dimensional organization: the *catalase fold*. Since then many other structures of heme enzymes capable of performing the catalase reaction have been determined including, less than a decade ago, the structures of the first heme containing catalase–peroxidases, which do not present the *catalase fold*. Despite the common catalytic features among these two families of unrelated heme enzymes, degrading efficiently hydrogen peroxide to water and oxygen in a two stage catalytic mechanism, mono-functional catalases and catalase–peroxidases present major differences in their kinetic and reactive properties. The increasing wealth of structural information available for all these heme-containing catalase enzymes is providing a consistent framework to understand and to study these systems. However, a number of major questions

remain unanswered that require continuing structural research with innovative approaches.

Acknowledgments

Many thanks are given to Prof. W. Melik-Adamyan for critical reading of the manuscript and for providing the image of the PVC model shown in Fig. 1. This work was supported in part by the Spanish Ministerio de Ciencia e Innovación (Grant BFU2009-09268, to I.F.), the Natural Sciences and Engineering Research Council of Canada (to P.C.L.), the Canada Research Chair Program (to P.C.L) and the Generalitat de Catalunya (BP-B2008-00239, to X.C.).

References

[1] J.B. Sumner, A.L. Dounce, Science 85 (1937) 366–367.
[2] B.K. Vainshtein, W.R. Melik-Adamyan, V.V. Barynin, V.V. Vagin, Y.V. Nekrasov, L.V. Malinina, M.F. Gulyi, L.V. Gudkova, R.G. Degtyar, Dokl Akad Nauk SSSR 246 (1979) 220–223.
[3] M.R. Murthy, T.J. Reid, A. Sicignano, N. Tanaka, M.G. Rossmann, J. Mol. Biol. 152 (1981) 465–499.
[4] T.J. Reid, M.R. Murthy, A. Sicignano, N. Tanaka, W.D. Musick, M.G. Rossmann, Proc. Natl. Acad. Sci. USA 78 (1981) 4767–4771.
[5] B.K. Vainshtein, W.R. Melik-Adamyan, V.V. Barynin, A.A. Vagin, A.I. Grebenko, Nature 293 (1981) 411–412.
[6] L.M. Foroughi, Y.N. Kang, A.J. Matzger, Acta Crystallogr. D: Biol. Crystallogr. 67 (2011) 756–762.
[7] A. Claiborne, I. Fridovich, J. Biol. Chem. 254 (1979) 4245–4252.
[8] B.L. Triggs-Raine, B.W. Doble, M.R. Mulvey, P.A. Sorby, P.C. Loewen, J. Bacteriol. 170 (1988) 4415–4419.
[9] X. Carpena, W. Melik-Adamyan, P.C. Loewen, I. Fita, Acta Crystallogr. D: Biol. Crystallogr. 60 (2004) 1824–1832.
[10] Y. Yamada, T. Fujiwara, T. Sato, N. Igarashi, N. Tanaka, Nat. Struct. Biol. 9 (2002) 691–695.
[11] X. Carpena, S. Loprasert, S. Mongkolsuk, J. Switala, P.C. Loewen, I. Fita, J. Mol. Biol. 327 (2003) 475–489.
[12] Y. Zhang, B. Heym, B. Allen, D. Young, S. Cole, Nature 358 (1992) 591–593.
[13] T. Bertrand, N.A.J. Eady, J.N. Jones, J. Biol. Chem. 279 (2004) 38991–38999.
[14] J. Bravo, I. Fita, P. Gouet, H.M. Jouve, W. Melik-Adamyan, G. Murshudov, J.G. Scandalios (Eds.), Cold Spring Harbor Laboratory Press, 1997.
[15] M. Zámocký, F. Koller, Prog. Biophys. Mol. Biol. 72 (1999) 19–66.
[16] M.J. Maté, G. Murshudov, J. Bravo, W. Melik-Adamyan, P.C. Loewen, I. Fita, A. Messerschmidt, R. Huber, T. Poulos, K. Wieghardt (Eds.), Wiley and Sons, Ltd., 2001.
[17] P. Nicholls, I. Fita, P.C. Loewen, Adv. Inorg. Chem. 51 (51) (2001) 51–106.
[18] P. Chelikani, I. Fita, P.C. Loewen, Cell Mol. Life Sci. 61 (2004) 192–208.
[19] H.N. Kirkman, G.F. Gaetani, Trends Biochem. Sci. 32 (2007) 44–50.
[20] M. Alfonso-Prieto, Doctoral Thesis, Barcelona (2009).
[21] G. Smulevich, C. Jakopitsch, E. Droghetti, C. Obinger, J. Inorg. Biochem. 100 (2006) 568–585.
[22] K.M. Manoj, L.P. Hager, Biochim. Biophys. Acta 1547 (2001) 408–417.
[23] K. Kühnel, W. Blankenfeldt, J. Terner, I. Schlichting, J. Biol. Chem. 281 (2006) 23990–23998.
[24] V.V. Barynin, A.A. Vagin, W.R. Melik-Adamyan, A.I. Grebenko, S.V. Khangulov, A.N. Popov, M.E. Adrianova, B.K. Vainshtein, Dokl Akad Nauk SSSR 288 (1986) 877–880.
[25] T.L. Poulos, Arch. Biochem. Biophys. 500 (2010) 3–12.
[26] M.G. Klotz, G.R. Klassen, P.C. Loewen, Mol. Biol. Evol. 14 (1997) 951–958.
[27] M.M. Horvath, N.V. Grishin, Proteins 42 (2001) 230–236.
[28] G.N. Murshudov, A.I. Grebenko, J.A. Brannigan, A.A. Antson, V.V. Barynin, G.G. Dodson, Z. Dauter, K.S. Wilson, W.R. Melik-Adamyan, Acta Crystallogr. D: Biol. Crystallogr. 58 (2002) 1972–1982.
[29] V. Jha, S. Louis, P. Chelikani, X. Carpena, L.J. Donald, I. Fita, P.C. Loewen, Biochemistry 50 (2011) 2101–2110.
[30] G.N. Murshudov, A.I. Grebenko, V. Barynin, Z. Dauter, K.S. Wilson, B.K. Vainshtein, W. Melik-Adamyan, J. Bravo, J.M. Ferrán, J.C. Ferrer, J. Switala, P.C. Loewen, I. Fita, J. Biol. Chem. 271 (1996) 8863–8868.
[31] P.C. Loewen, J. Switala, A. Von Ossowski, A. Hillar, B. Christie, P. Tattrie, Biochemistry 32 (1993) 10159–10164.
[32] C. Obinger, M. Maj, P. Nicholls, P. Loewen, Arch. Biochem. Biophys. 342 (1997) 58–67.
[33] I. Fita, M.G. Rossmann, J. Mol. Biol. 185 (1985) 21–37.
[34] P. Loewen, Gene 179 (1996) 39–44.
[35] W. Melik-Adamyan, J. Bravo, X. Carpena, J. Switala, M.J. Maté, I. Fita, P.C. Loewen, Proteins 44 (2001) 270–281.
[36] S.G. Kalko, J.L. Gelpí, I. Fita, M. Orozco, J. Am. Chem. Soc. 123 (2001) 9665–9672.
[37] M. Alfonso-Prieto, X. Biarnés, P. Vidossich, C. Rovira, J. Am. Chem. Soc. 131 (2009) 11751–11761.
[38] P. Chelikani, X. Carpena, I. Fita, P.C. Loewen, J. Biol. Chem. 278 (2003) 31290–31296.
[39] C.D. Putnam, A.S. Arvai, Y. Bourne, J.A. Tainer, J. Mol. Biol. 296 (2000) 295–309.
[40] L. Domínguez, A. Sosa-Peinado, W. Hansberg, Arch. Biochem. Biophys. 500 (2010) 82–91.
[41] M.S. Sevinc, M.J. Maté, J. Switala, I. Fita, P.C. Loewen, Protein Sci. 8 (1999) 490–498.
[42] H.N. Kirkman, G.F. Gaetani, Proc. Natl. Acad. Sci. USA 81 (1984) 4343–4347.
[43] H.N. Kirkman, S. Galiano, G.F. Gaetani, J. Biol. Chem. 262 (1987) 660–666.
[44] L.P. Olson, T.C. Bruice, Biochemistry 34 (1995) 7335–7347.
[45] W. Sicking, H.-G. Korth, H. de Groot, R. Sustmann, J. Am. Chem. Soc. 130 (2008) 7345–7356.
[46] J. Bravo, M.J. Mate, T. Schneider, J. Switala, K. Wilson, P.C. Loewen, I. Fita, Proteins 34 (1999) 155–166.
[47] M. Alfonso-Prieto, A. Borovik, X. Carpena, G. Murshudov, W. Melik-Adamyan, I. Fita, C. Rovira, P.C. Loewen, J. Am. Chem. Soc. 129 (2007) 4193–4205.
[48] P.C. Loewen, X. Carpena, C. Rovira, A. Ivancich, R. Pérez-Luque, R. Haas, S. Odenbreit, P. Nicholls, I. Fita, Biochemistry 43 (2004) 3089–3103.
[49] I. Fita, A.M. Silva, M.R. Murthy, M.G. Rossmann, Acta Crystallogr. B 42 (1986) 497–515.
[50] M.L. Oldham, A.R. Brash, M.E. Newcomer, Proc. Natl. Acad. Sci. USA 102 (2005) 297–302.
[51] S. Pakhomova, B. Gao, W.E. Boeglin, A.R. Brash, M.E. Newcomer, Protein Sci. 18 (2009) 2559–2568.
[52] K.G. Welinder, J.M. Mauro, L. Nørskov-Lauritsen, Biochem. Soc. Trans. 20 (1992) 337–340.
[53] M. Wilming, K. Johnsson, FEBS Lett. 509 (2001) 272–276.
[54] L.J. Donald, O.V. Krokhin, H.W. Duckworth, B. Wiseman, T. Deemagarn, R. Singh, J. Switala, X. Carpena, I. Fita, P.C. Loewen, J. Biol. Chem. 278 (2003) 35687–35692.
[55] R.A. Ghiladi, G.M. Knudsen, K.F. Medzihradszky, J. Biol. Chem. 280 (2005) 22651–22663.
[56] B. Wiseman, X. Carpena, M. Feliz, L.J. Donald, M. Pons, I. Fita, P.C. Loewen, J. Biol. Chem. 285 (2010) 26662–26673.
[57] T. Deemagarn, B. Wiseman, X. Carpena, A. Ivancich, I. Fita, P.C. Loewen, Proteins 66 (2007) 219–228.
[58] X. Carpena, B. Wiseman, T. Deemagarn, R. Singh, J. Switala, A. Ivancich, I. Fita, P.C. Loewen, EMBO Rep. 6 (2005) 1156–1162.
[59] R. Singh, J. Switala, P.C. Loewen, A. Ivancich, J. Am. Chem. Soc. 129 (2007) 15954–15963.
[60] P. Vidossich, M. Alfonso-Prieto, X. Carpena, P.C. Loewen, I. Fita, C. Rovira, J. Am. Chem. Soc. 129 (2007) 13436–13446.
[61] P. Vidossich, X. Carpena, P.C. Loewen, I. Fita, C. Rovira, J. Phys. Chem. Lett. 2 (2011) 196–200.
[62] J. Suarez, K. Ranguelova, A.A. Jarzecki, J. Manzerova, V. Krymov, X. Zhao, S. Yu, L. Metlitsky, G.J. Gerfen, R.S. Magliozzo, J. Biol. Chem. 284 (2009) 7017–7029.
[63] R.D. Baker, C.O. Cook, D.C. Goodwin, Biochemistry 45 (2006) 7113–7121.
[64] B.K. Vainshtein, W.R. Melik-Adamyan, V.V. Barynin, A.A. Vagin, A.I. Grebenko, V.V. Borisov, K.S. Bartels, I. Fita, M.G. Rossmann, J. Mol. Biol. 188 (1986) 49–61.
[65] I. Fita, M.G. Rossmann, Proc. Natl. Acad. Sci. USA 82 (1985) 1604–1608.
[66] J. Bravo, N. Verdaguer, J. Tormo, C. Betzel, J. Switala, P.C. Loewen, I. Fita, Structure 3 (1995) 491–502.
[67] M.J. Maté, M. Zamocky, L.M. Nykyri, C. Herzog, P.M. Alzari, C. Betzel, F. Koller, I. Fita, J. Mol. Biol. 286 (1999) 135–149.
[68] G.N. Murshudov, W.R. Melik-Adamyan, A.I. Grebenko, V.V. Barynin, A.A. Vagin, B.K. Vainshtein, Z. Dauter, K.S. Wilson, FEBS Lett. 312 (1992) 127–131.
[69] X. Carpena, M. Soriano, M.G. Klotz, H.W. Duckworth, L.J. Donald, W. Melik-Adamyan, I. Fita, P.C. Loewen, Proteins 50 (2003) 423–436.
[70] K.O. Håkansson, M. Brugna, L. Tasse, Acta Crystallogr. D: Biol. Crystallogr. 60 (2004) 1374–1380.
[71] A. Díaz, E. Horjales, E. Rudiño-Piñera, R. Arreola, W. Hansberg, J. Mol. Biol. 342 (2004) 971–985.
[72] P. Chelikani, X. Carpena, R. Perez-Luque, L.J. Donald, H.W. Duckworth, J. Switala, I. Fita, P.C. Loewen, Biochemistry 44 (2005) 5597–5605.
[73] I. Hara, N. Ichise, K. Kojima, H. Kondo, S. Ohgiya, H. Matsuyama, I. Yumoto, Biochemistry 46 (2007) 11–22.
[74] E.K. Riise, M.S. Lorentzen, R. Helland, A.O. Smalås, H.-K.S. Leiros, N.P. Willassen, Acta Crystallogr. D: Biol. Crystallogr. 63 (2007) 135–148.
[75] A. Díaz, V.-J. Valdés, E. Rudiño-Piñera, E. Horjales, W. Hansberg, J. Mol. Biol. 386 (2009) 218–232.
[76] A.A. Borovik, A.I. Grebenko, W.R. Melik-Adamyan, Krystallografiya 56 (2011) 635–640.
[77] E. Peña-Soler, M.C. Vega, M. Wilmanns, C. Williams, Acta Crystallogr. D: Biol. Crystallogr. 67 (2011) 690–698.
[78] T. Deemagarn, X. Carpena, R. Singh, B. Wiseman, I. Fita, P.C. Loewen, J. Mol. Biol. 345 (2005) 21–28.
[79] X. Zhao, H. Yu, S. Yu, F. Wang, J.C. Sacchettini, R.S. Magliozzo, Biochemistry 45 (2006) 4131–4140.
[80] X. Carpena, B. Wiseman, T. Deemagarn, B. Herguedas, A. Ivancich, R. Singh, P.C. Loewen, I. Fita, Biochemistry 45 (2006) 5171–5179.
[81] P. Gouet, H.M. Jouve, O. Dideberg, J. Mol. Biol. 249 (1995) 933–954.